Nucleic Acids Research, 1997, Vol. 25, No. 14 **2923–2929**

Stability, specificity and fluorescence brightness of multiply-labeled fluorescent DNA probes

John B. Randolph* and Alan S. Waggoner+

Center for Light Microscope Imaging and Biotechnology and Department of Chemistry, Carnegie Mellon University, 4400 Fifth Avenue, Pittsburgh, PA 15213, USA

Received November 27, 1996; Revised and Accepted May 27, 1997

ABSTRACT

In this work, we studied the fluorescence and hybridization of multiply-labeled DNA probes which have the hydrophilic fluorophore 1-(ε-carboxypentynyl)-1′-ethyl-3,3,3′,3′-tetramethylindocarbocyanine-5,5′-disulfonate (Cy3) attached via either a short or long linker at the C-5 position of deoxyuridine. We describe the effects of labeling density, fluorophore charge and linker length upon five properties of the probe: fluorescence intensity, the change in fluorescence upon duplex formation, the quantum yield of fluorescence (Φ_f), probe–target stability and specificity. For the hydrophilic dye Cy3, we have demonstrated that the fluorescence intensity and Φ_f are maximized when labeling every 6th base using the long linker. With a less hydrophilic dye, a labeling density this high could not be achieved without serious quenching of the fluorescence. The target specificity of multiply-labeled DNA probes was just as high as compared to the unmodified control probe, however, a less stable probe–target duplex is formed that exhibits a lower melting temperature. A mechanism that accounts for this destabilization is proposed which is consistent with our data. It involves dye–dye and dye–nucleotide interactions which appear to stabilize a single-stranded conformation of the probe.

INTRODUCTION

Fluorescent DNA probes for *in situ* hybridization are now commonly used in a wide spectrum of applications such as the determination of mRNA distributions on the cellular and subcellular level (1,2), monitoring gene expression (3,4), detecting gene deletions and translocations (5–7), detecting chromosome translocations (8) and the mapping (9–11) and sequencing (12,13) of genes. Increasing the detection sensitivity would allow even greater application of this method. The main factors that determine the sensitivity of a fluorescent DNA probe are its brightness, target specificity and the stability of the probe–target duplex. Previously, DNA or RNA probes were either chemically labeled with only a single fluorophore on the 5′ end of the oligonucleotide (12,14) or were labeled by enzymatic means, such as nick translation or *in vitro* transcription, which incorporates dye-modified nucleotides for, on average, 4% of the bases (15,16). Current technology now allows multiple fluorescent labels to be directly attached to the oligomer by chemical means which may lead to brighter probes (17–19). However, increasing the labeling density of the fluorophore has been shown not to necessarily increase the sensitivity of the probe (20), since it also is known to quench fluorescence, reduce the extinction coefficient of the dyes (21,22) and decrease the stability of the probe–target duplex (17,23). The amount of destabilization is dependent upon the site used for attaching the dye. Some locations for covalent dye attachment, such as the sugar, via a modified 2′-aminonucleoside (24), or the phosphate backbone, via the use of phosphorothioates (25), have been shown to result in significant duplex destabilization even at a low degree of dye incorporation.

In this work, we have synthesized a series of DNA probes that are multiply labeled with either the disulfonated, anionic fluorophore Cy3, or a mono-sulfonated, zwitterionic Cy3 analogue, Cy3NOS. The oligonucleotides were 27mers of thymidine with dye-labeled deoxyuridine analogues evenly spaced throughout the oligonucleotide. Fluorophores were covalently attached to linkers at the C-5 position of deoxyuridine analogues where the effect upon hybridization should be minimal (17). Two linker lengths were studied. By using the 27dT sequence for our probes, dyes could be attached to the oligonucleotide without any sequence constraints and the duplex stability of the probes could be compared directly by determination of the melting temperature (T_m). The probe specificity was measured through ΔT_m measurements, defined as the difference between T_m values of the probe annealed to DNA target with respect to when annealed to a single-base mismatched target (26).

We report the effect of labeling density, fluorophore charge and linker length upon fluorescence intensity, the change in fluorescence upon duplex formation, the quantum yield of fluorescence (Φ_f), and probe-target stability and specificity.

MATERIALS AND METHODS

Dye synthesis and characterization

The active *N*-hydroxysuccinimidyl (NHS) esters of Cy3 and Cy3NOS (Fig. 1A) used to label the oligonucleotides were synthesized according to the procedure of Mujumdar (27). Cy3NOS was obtained by using the non-sulfonated intermediate 1-(ε-carboxypentynyl)-2,3,3-trimethylindolenium iodide (a generous gift of Dr Mark Reddington) to produce the zwitterionic Cy3 analogue. The crude Cy3NOS was purified on a C18 reverse phase column using 15% MeOH as the eluant. Salts that co-eluted

*To whom correspondence should be addressed at present address (as of September 1, 1997): Glen Research Corporation, 44901 Falcon Place, Sterling, VA 20166, USA. Tel: +1 703 437 6191; Fax: +1 703 435 9774; Email: jr4h@andrew.cmu.edu

+Present address: Amersham Life Sciences, 955 William Pitt Way, Pittsburgh, PA 15238, USA

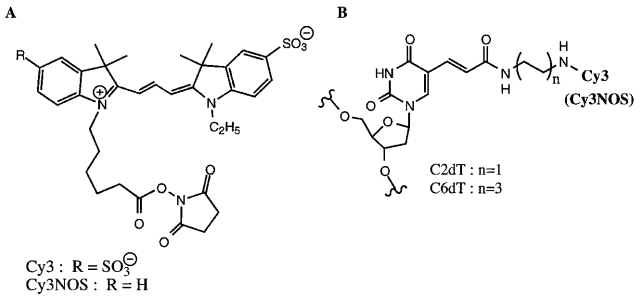

C

Probe	Sequence
27dT	T T T T T T T T T T T T T T T T T T T T T T T T T
42	**T*** T T T T T **T*** T T T T T **T*** T T T T T **T*** T T T T T
46	**T°** T T T T T **T°** T T T T T **T°** T T T T T **T°** T T T T T
52	**T*** T T T T **T*** T T T T **T*** T T T T **T*** T T T T **T*** T T
56	**T°** T T T T **T°** T T T T **T°** T T T T **T°** T T T T **T°** T T
62	**T*** T T T **T*** T T T **T*** T T T **T*** T T T **T*** T T T **T*** T
66	**T°** T T T **T°** T T T **T°** T T T **T°** T T T **T°** T T T **T°** T
27dA	A A A A A A A A A A A A A A A A A A A A A A A A A
26A1G	A A A A A A A A A A A A A **G** A A A A A A A A A A A

Figure 1. (**A**) The structures of Cy3 and Cy3NOS. (**B**) The structure of the amino-modified uridine analogues, C2dT and C6dT, when coupled to the dyes Cy3 and Cy3NOS. (**C**) Sequences of the DNA probes used in this study. **T*** and **T°** mark the positions where the modified bases C2dT and C6dT have been incorporated respectively. The probes were designated by a two digit code. The first digit indicates the number of dyes attached and the second, which modified base was used: '2' and '6' for C2dT and C6dT respectively. Unless explicitly stated otherwise, all probes were labeled with Cy3. One probe, 56NOS, was labeled with Cy3NOS rather than Cy3.

with the Cy3NOS were removed by triturating the product over water. The structures of the Cy3 and Cy3NOS were confirmed by ^{1}H NMR. The Cy3NOS had an extinction coefficient (ε) of 135 000 l/mol·cm at its λ_{max} 546 nm and a Φ_f of 0.046 in 10% MeOH determined against a Rhodamine 6G standard in EtOH. The ε_{550} and Φ_f for Cy3 are 150 000 and 0.04 respectively (27). The dyes were converted to the NHS ester (27), dissolved in dry dimethylformamide (DMF) and stored at 4°C over activated 3 Å molecular sieves until use. The water solubility of the Cy3NOS carboxylic acid was found to be 4.53×10^{-4} M (0.249 g/l) at room temperature as determined by absorbance. For Cy3 carboxylic acid, the water solubility was >0.34 M (234 g/l).

Oligonucleotide synthesis, labeling and purification

The modified bases were introduced into the oligonucleotides using the phosphoramidites amino-modifier C2dT and amino-modifier C6dT (Glen Research). The fluorophores were attached through the formation of an amide bond between the primary amine of linker and the active *N*-hydoxysuccinimidyl ester of the dye. Figure 1B shows the structures of C2dT and C6dT labeled with Cy3 and Cy3NOS.

The oligonucleotides used in this study (Fig. 1C) were synthesized on a Gene Assembler Plus (Pharmacia LKB) on a 0.2 µM synthesis scale using Pharmacia reagents and were deprotected using standard procedures (3).

The labeling conditions used for probe 42 are as follows: 90 nmol of unlabeled probe 42 was dried by speedvac and taken up in 360 µl of 0.5 M carbonate/bicarbonate buffer, pH 9.5 (Buffer A). A 53 µl aliquot of a 135 mM solution of Cy3 NHS ester in DMF was evaporated to a glass (speedvac), taken up in 20 µl dH_2O and

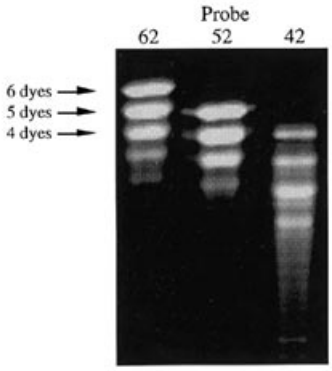

Figure 2. Fluorescence image of an acrylamide gel showing typical product distribution after labeling probes 42, 52 and 62 with Cy3.

immediately added to the oligonucleotide solution, which was vortexed and kept overnight at room temperature. For probes 42 and 46, 20 dye equivalents per amino group were used. For the 52/56 and 62/66 probes, 30 and 40 dye equivalents per amino group were used respectively. For probe 56NOS, a 90 nmol sample of unlabeled probe 56 was taken up in 360 µl of Buffer A. To this, 255 µl of Cy3NOS NHS ester in dry DMF, equivalent to 30 dyes per amino group, was added and the reaction mixture was vortexed for 10 min. After labeling with either Cy3 or Cy3NOS, the free dye was removed from the labeled oligomer by gel-filtration through a 20 cm column of BioGel P4 (Bio-Rad) equilibrated with 0.1 M triethylammonium acetate.

Generally, 85% labeling was observed per amino group which leads to a distribution of multiply-labeled probes (Fig. 2). The slowest running band in each lane is the fully labeled oligonucleotide. The successively faster bands correspond to the *n*–1, *n*–2 and *n*–3 partially labeled probes, where *n* is the number of modified bases present.

The probes were purified by polyacrylamide gel electrophoresis (PAGE) on 20% acrylamide gels containing 7 M urea and 5% bisacrylamide (28). The slowest running band was excised and the oligomer was extracted by the 'crush-and-soak' method as described (28) with the exceptions that the elution buffer contained no SDS and the elution was carried out at room temperature overnight. The oligomers were recovered on a Sep-Pak C18 column (28). Three consecutive gels were required to obtain a pure probe. Unlabeled probes 42–66, as well as the unmodified oligonucleotides 27dT, 27dA and 26A1G, were also purified by PAGE, though only a single run was performed. A single band was observed by UV shadowing and excised.

MALDI mass spectrometry was used to confirm the structures of both a Cy3-labeled probe (probes 46) and a Cy3NOS-labeled probe (56NOS). For probe 46, the expected molecular weight was 11219 and the observed m/z ratio found was 11178. For probe 56NOS, the expected molecular weight was 11585 and the observed m/z ratio found was 11589. The results were within 0.36 and 0.012% of the calculated molecular weights respectively.

Extinction coefficient of probes

The extinction coefficients (ε) of the probes were determined in 10 mM Tris–$HClO_4$ at pH 7.0 according to the method of Cantor and Tinoco (29). The experiments were performed in duplicate for each labeled probe and the results were within 2%. The results are listed in Table 1. The extinction coefficients at 260 nm used

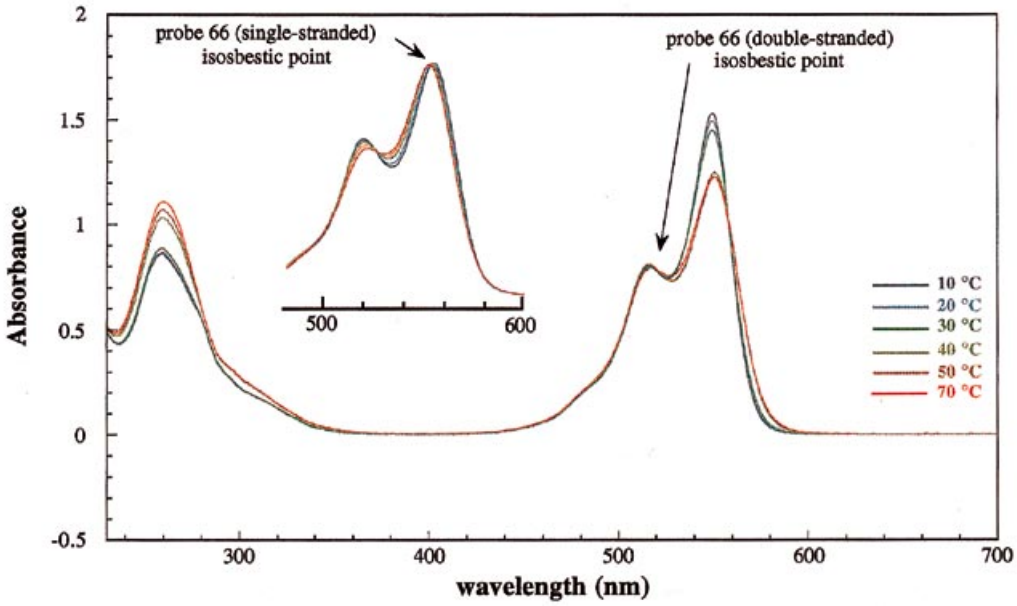

Figure 3. Absorbance spectra of probe 66 annealed to poly[dA] from 10 to 70°C showing that the extinction coefficient of the dyes is sensitive to the conformation of the probe. The absorbance at 551.4 nm drops abruptly between 30 and 40°C as probe 66 passes through the transition from being double-stranded to being single-stranded. The single-stranded probe shows no such transition (inset).

for the nucleotides were 9110 (pdT), 15300 (pdA) and 11800 (pdG) all in l/mol·cm (30). The ε of C2dT and C6dT were taken as 119% of dT (Hugh Mackie, Glen Research, personal communication) yielding a value of 10800. For pdT and pdG, the literature values listed are for 268 nm (pH 7) and 255 nm (pH 1) respectively. These were extrapolated to 260 nm, pH 7.0, by determining the ratio of the absorbance at 268 nm (pH 7) and 255 nm (pH 1) for pdT and pdG to the absorbance of the nucleotides at 260 nm, pH 7.0. With multiple dyes attached, there is a significant contribution by the dyes to the absorbance at 260 nm. Therefore, the absorbance of the dyes at 260 nm was taken into account (4900 and 9000 l/mol·cm per dye attached for Cy3 and Cy3NOS respectively).

Table 1. The extinction coefficients of the probes, in $l \cdot mol^{-1} \cdot cm^{-1}$

Probe	$\varepsilon 260 \times 10^{-5}$ unlabeled	$\varepsilon 260 \times 10^{-5}$ Cy3-labeled	$\varepsilon 552 \times 10^{-5}$ Cy3-labeled
27T	2.15	–	–
27dA	3.63	–	–
26A1G	3.60	–	–
42	2.44	2.64	5.77
46	2.49	2.66	5.71
52	2.45	2.69	6.85
56	2.50	2.72	6.74
62	2.47	2.77	8.03
66	2.52	2.82	7.87

Due to differences between the Cy3 and Cy3NOS dyes, the extinction coefficients of probe 56NOS are significantly different at 260 and 550 nm, 2.78 and 5.10 ($\times 10^{-5}$) respectively.

Melting curves

Melting curves were obtained on an Aviv 14DS UV-vis Spectrophotometer (Aviv) fitted with a thermoelectric temperature-controlled cell holder. The cuvette jacket temperature was monitored concurrently with the absorbance at 260 and 551.4 nm.

The wavelength 551.4 nm was chosen because it was found to be an isosbestic point for probe 66 when single-stranded (Fig. 3, inset). Absorbance spectra of probe 66 in 100 mM NaCl, 10 mM Na cacodylate pH 7.0, 25°C (Buffer B) were taken from 10 to 70°C at 10°C intervals from which the isosbestic wavelength was determined. By choosing to monitor this wavelength during the melting curve determination of double-stranded probes, the change in the absorbance of the dyes should be due to conformational changes in the DNA and not due to the effect of changes in temperature upon the dye itself.

The melting curves were determined as follows: 0.63 nmol of both probe and target (either the matching target 27dA or the mismatching target 26A1G) were combined and dried by speedvac. The sample was taken up in 550 µl Buffer B to yield a total strand concentration of 2.29×10^{-6} M. The solution was warmed to 50°C and gradually cooled to 4°C where it was maintained until the melting experiment was performed. Samples (0.5 ml) of annealed probe were ramped at 1°C/min from 0 to 70°C, held for 2 min at 70°C and ramped back down to 0°C. Data were collected every 60 s, with each datum the average of 10 points collected over 1 s. The spectral bandwidth was 1 nm.

The lag between the true cuvette temperature and the monitored jacket temperature was corrected for by calibration using optical thermometry (31). In addition, melting curves were determined for Buffer B alone to account for any changes in buffer absorbance with temperature. These 260 and 551.4 nm melting curves were fitted to 4th order polynomials which were used to generate melting curves of the buffer at 260 and 551.4 nm for any given temperature ramp. These estimated curves were subtracted from

the melting curve of the probe, correcting for the change in background absorbance with temperature. The melting temperature (T_m) was determined by finding the inflection point of the absorbance curve at 260 nm from the derivative curve, $\partial A/\partial T$, smoothed over 5 points.

Data for probe 66 is not listed as the probe bound irreversibly to a 0.2 µm Millex-GS filter (Millipore). Previous work in our lab with probe 66 using poly[dA] as the target indicated that the T_m and fluorescence data followed the same trend as probe 62.

Quantum yield of fluorescence

The Φ_f of the hybridized probes were determined with a SPEX Fluorolog II spectrofluorometer (SPEX Industries, Inc.) fitted with a temperature controlled cuvette holder and using rhodamine 6G in EtOH as the standard according to O'Brien (32). The excitation wavelength was 514.5 nm which allows the entire emission spectra of the Rhodamine 6G, Cy3 and Cy3NOS to be observed. The emission was scanned from 516 to 800 nm with 1 nm increments, 1 s integration time with all slit widths at 0.5 mm. The annealed probes, previously used to determine the melting curves, were diluted with Buffer B such that their absorbances were 0.05 at 514.5 nm. Prior to the fluorescence measurements, the annealed probes were equilibrated at 21.5°C for 10 min. Fluorescence brightness was defined as the integrated peak area from 516 to 800 nm, correcting for probe concentration.

Percent change in fluorescence upon hybridization

To determine the effect of hybridization upon fluorescence, equimolar solutions of probe at 21.5°C, with and without poly[dA] target, were excited at 520.4 nm and the fluorescence emission was observed from 527.4 to 724.4 nm.

To ensure that the changes in fluorescence intensity measured were not due to changes in the extinction coefficient of the dyes caused by differences in probe hybridization, a second isosbestic point was determined at which the dye absorbance is the same regardless of whether the probe is single- or double-stranded (Fig. 3). By using this isosbestic point at 520.4 nm for the excitation wavelength, the fluorescence enhancement measurements should be a function of the Φ_f only.

The percent change in fluorescence upon hybridization with target was determined as follows: 0.0546 nmol of probe was taken up in 4.2 ml of Buffer B, yielding a concentration of 1.30×10^{-8} M. From this solution, 2 ml were transferred to two matched quartz cuvettes. To one cuvette, 1.36 µl of poly[dA] (average length 300 nucleotides) was added. The dA concentration was 0.516 mM, which yielded a 1:1 nucleotide ratio of probe to target. The cuvettes were then sealed with teflon stoppers, shaken, warmed to 50°C and allowed to anneal for at least 6 h, slowly cooling to 4°C. The samples were excited at 520.4 nm and scanned from 527.4 to 724.4 nm, with the excitation and emission slit widths at 2 mm. Two measurements were taken for each probe before and after 50% dilution with buffer which was added directly to the cuvette. For probes 42, 52, 56 and 56NOS the experiments were repeated. The fluorescence determined was the peak area from 527.4 to 724.4 nm. The percent change in fluorescence upon duplex formation reported is defined as $[[I_f(ds) - I_f(ss)]/I_f(ss)] \times 100$.

It was found that annealing the probes in polypropylene tubes and then transferring the solutions to cuvettes yielded erroneous results due to differential adhesion of the single- versus double-stranded probes to the polypropylene tube. Therefore, the probes were annealed within the cuvettes to avoid any transferring and loss of oligonucleotide.

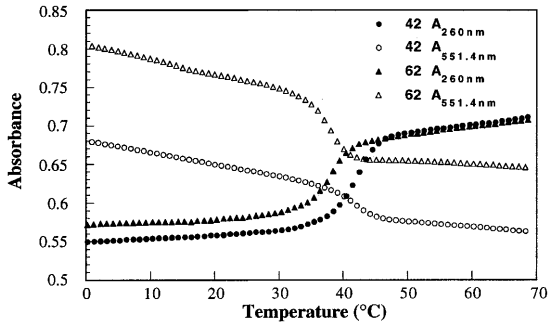

Figure 4. Examples of the melting curves obtained. Shown are the superimposed melting curves of probes 42 and 62 when bound to 27dA, observed at 260 and 551.4 nm from 0 to 70°C. For clarity, the melting curves from 70 to 0°C are not shown, however, little hysteresis was observed.

RESULTS

Duplex stability and specificity

All the probes exhibited normal melting behavior. Figure 4 shows the melting curves for probes 42 and 62 which represent the low and high dye-labeling densities investigated in this study (four and six dyes per oligomer respectively). It is apparent that even when the labeling density on the probe is as high as every 5th base (probe 62), the duplex still melts in a cooperative manner with little broadening of the transition. That transition, however, has been shifted to a lower temperature compared to probe 42. In addition, the transition from duplex to single-stranded DNA is reflected in the absorbance curve of the dye as well as the oligonucleotide absorbance at 260 nm.

The melting temperatures of the probes annealed to the matching target 27dA and to the mismatch target 26A1G were determined (Table 2). From these data, we make four observations: (i) each additional negatively-charged Cy3 reduces the T_m by ~2°C; (ii) the zwitterionic Cy3NOS destabilizes the helix more than an equivalent number of Cy3 labels do; (iii) extending the linker length by four carbons does not appreciably alter the T_m and (iv) since ΔT_m is the change in stability of the duplex when one mismatch is present (which is measure of probe specificity), the probe specificity does not change significantly with dye labeling.

The reduction in the T_m is not due to the incorporation of amino-modified uridine analogues *per se*; melting curve determinations for the six probes 42–66 indicated that there is no decrease in the T_m prior to labeling with Cy3 (data not shown).

Fluorescence intensity, quantum yield and the effect of duplex formation

The fluorescence intensity of the hybridized Cy3-labeled probes initially increases as additional dyes are added (Table 2). Once six dyes are attached, however, the intensity decreases. The same trend is seen with the quantum yield of fluorescence (Φ_f). Both the fluorescence and Φ_f are relatively insensitive to the presence of a mismatch and the length of the linker.

Table 2. The melting temperatures, Φ_f and fluorescence brightness of the probes when bound to the target probes 27dA (match) or 26A1G (mismatch)

Probe	T_m (°C)		ΔT_m	Φ_f		Fluorescence intensity	
	Match	Mis-match	–	Match	Mis-match	Match	Mis-match
27T	49.7	44.9	4.8	–	–	–	–
42	41.5	37.0	4.5	0.09	0.09	7.8	8.1
46	41.6	37.0	4.6	0.09	0.09	7.5	7.6
52	40.5	35.7	4.8	0.10	0.12	10.1	11.1
56	40.6	35.4	5.2	0.11	0.11	9.9	10.0
56NOS	37.6	32.9	4.7	0.06	0.07	4.9	6.6
62	37.6	–	–	0.09	–	8.9	–

The error in the T_m, Φ_f and fluorescence are 0.2, 0.01 and 0.1 respectively.

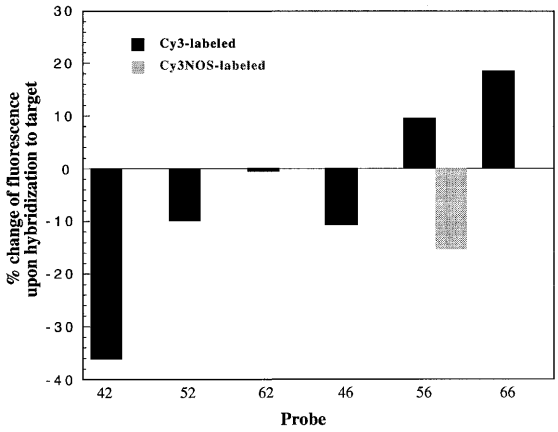

Figure 5. Percent change in fluorescence observed for probes upon hybridization to target.

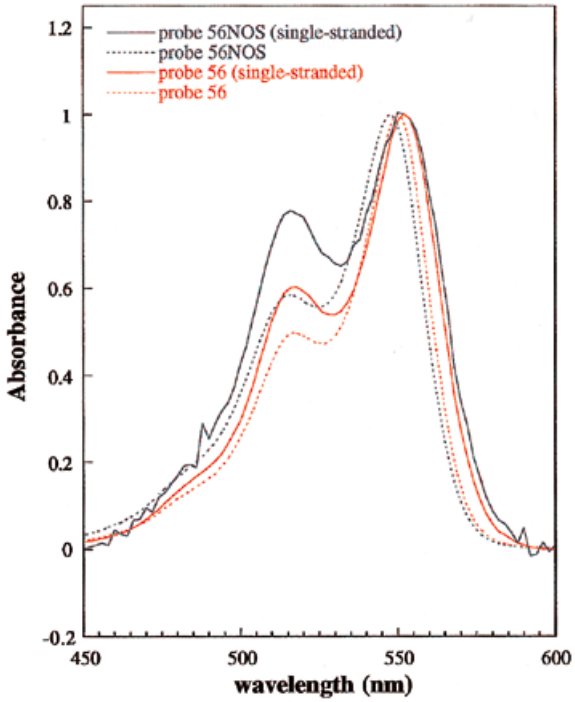

Figure 6. Absorbance spectra of probes 56 and 56NOS when double- and single-stranded. The magnitude of the absorbance of the shoulder at 515 nm indicates the degree of dye dimer present. The spectra were normalized at the dye monomer band at 550 nm.

The 56NOS probe showed a 50% drop in fluorescence and Φ_f compared to probe 56 even though the two probes share the same sequence, label density and linker length. Other than the additional sulfonate on Cy3, the labels themselves are very similar both structurally and spectroscopically. However, the presence of the additional sulfonate produces a large difference in water solubility.

Hybridization to target DNA significantly affects the fluorescence intensity of the probes (Fig. 5). The percent change in fluorescence upon duplex formation ranges from –35 to +20 for probes 42 and 66 respectively. Whether the fluorescence increases or decreases upon duplex formation depends upon labeling density, fluorophore charge and linker length. Probes that are labeled at low density, have short linkers, or are labeled with Cy3NOS, exhibit less fluorescence when hybridized. Only probes 56 and 66 show greater fluorescence in double-stranded structures.

DISCUSSION

Mechanisms of duplex destabilization

One of the conspicuous effects of multiple labeling of DNA oligonucleotides with the cyanine dyes is the degree to which it lowers the T_m. The source of this destabilization appears to arise from dye–dye and dye–nucleotide interactions.

There is evidence that dye–dye interactions are present in the probes. The H-aggregate is the most common dye–dye aggregate which, in its simplest form, is a stacked dye dimer whose formation is characterized by a decrease in the monomeric dye absorption band and an increase in a non-fluorescent, blue-shifted H-band (33). A comparison was made between probes 56 and 56NOS when single- and double-stranded (Fig. 6). The increase in the 515 nm band relative to the 0 → 0 transition of the monomer at 550 nm is characteristic of the presence of dye dimer (21,33). Probe 56NOS shows a pronounced H-band compared to probe 56. This is not surprising considering the low water solubility of the Cy3NOS label which favors dye aggregation. As previously noted, the transition from duplex to single-stranded DNA is reflected in both the oligonucleotide and dye absorbance curves (Fig. 4). The drop in dye absorbance upon duplex melting is most easily explained by H-aggregate formation, since an increase in the H-band will be at the expense of the monomer absorption band. Since dimerization is favored when the probes are single-stranded (Fig.6), the decrease in dye absorbance should be centered around the T_m, which is what is observed.

Dye dimer formation will affect the stability of the probe–target duplex. Dimer formation is an exothermic process, on the order

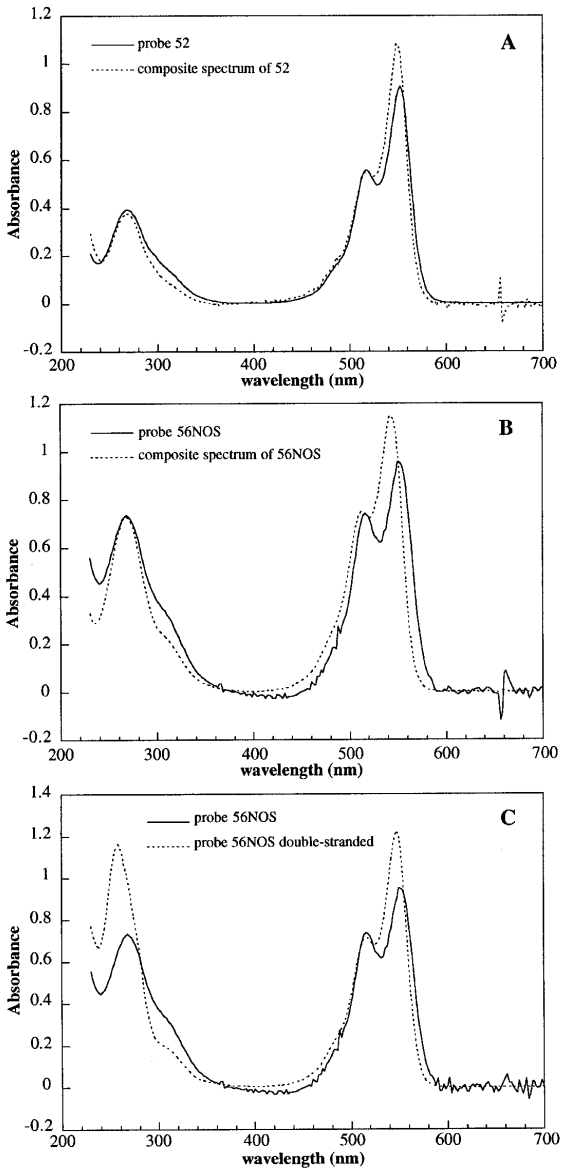

Figure 7. (**A**) The absorbance spectrum of probe 52 and its calculated composite spectrum when no dye–nucleotide or dye–dye interactions are present. The increase in the absorbance of the shoulder at 310 nm suggests that the presence of the dyes do perturb the nucleotide bases and that dye–nucleotide interactions are significant. (**B**) The absorbance spectrum of probe 56NOS and its calculated composite spectrum when no dye–nucleotide or dye–dye interactions are present. The more pronounced shoulder at 310 nm suggests that the zwitterionic dye Cy3NOS interacts more than the anionic dye Cy3 with the nucleotides. (**C**) Spectra of equimolar solutions of probe 56NOS when single-stranded and double-stranded. Note that the shoulder at 310 nm decreases upon addition of DNA target, suggesting that formation of the double helix disrupts the dye–nucleotide interactions. In addition, the double-stranded absorbance spectrum begins to look very similar to the composite spectrum of probe 56NOS when no dye–nucleotide or dye–dye interactions are present (B). The composite spectra were calculated by (i) recording spectra of the probes when labeled with dyes and unlabeled; (ii) the spectra of the free dyes were recorded and the baselines were corrected; (iii) the spectra of the unlabeled probes were normalized against the labeled probes to give spectra for identical probe concentrations; (iv) the spectra of the free Cy3 and Cy3NOS were normalized against the probes at the isosbestic point between the monomer and dimer forms (520.4 nm) to yield identical dye concentrations; and (v) the spectra of the corrected dyes and unlabeled probes were added to give the composite spectra of 52 and 56NOS.

of 25 kJ/mol at 25°C for most dyes (33). Since dimerization is favored when the probes are single-stranded, dye–dye interactions would be expected to stabilize a single-stranded conformation of the DNA probe. This would shift the equilibrium away from duplex formation and lead to a lower T_m. This model predicts that, as more dyes are added to a DNA probe, the oligomer will increasingly be locked into non-fluorescent, single-stranded conformations, lowering the duplex stability of the probe. This trend is observed in Table 2. Another prediction of this model is that upon addition of target to single-stranded probe, the fluorescence should go up. As seen in Figure 5, however, this is true for only two of the probes. Therefore, though it appears that dye dimer formation does contribute to the destabilization of the probe–target duplex, other effects must also be taken into account.

Dye–nucleotide interactions could be another possible explanation of the observed duplex destabilization. Recently it has been reported that with singly-labeled fluorescent DNA probes, dye–DNA interactions are present as observed by fluorescence anisotropy and fluorescence lifetimes (34). Such interactions would have to be broken to form a double helix and therefore, one would expect a monotonic decrease in the T_m as more dyes are attached.

We have used absorption spectroscopy to look for evidence of dye–nucleotide interactions. Significant ground state dye–nucleotide interactions may have an effect upon the UV absorbance spectrum of the oligonucleotide. If this is the case, the spectrum of a labeled probe will not equal its composite spectrum obtained by adding the spectrum of the free dye (carboxylate form) to the spectrum of the unlabeled DNA oligomer. We can exclude dye–dye interactions (present in the single-stranded probe) as a major contributor to any difference in the absorbance in the UV region because, although there is a 14% decrease in absorbance at 280 nm upon dimer formation, between 295 and 315 nm there is essentially no change in the dye absorbance spectra (data not shown). Therefore, at least in the region between 295 and 315 nm, actual and composite spectral changes are most likely due to dye–nucleotide interactions. The composite and actual spectra for probes 56NOS and 52 are shown in Figure 7.

There are significant differences between the actual spectra of probes 56NOS and 52 and their respective composite spectra for which no dye–nucleotide or dye–dye interactions are present (Fig. 7A and B). The increase in the absorbance of the shoulder at 310 nm suggests that the presence of the Cy3 dyes do perturb the nucleotide bases and that dye–nucleotide interactions are significant. In Figure 7B, the more pronounced shoulder at 310 nm suggests that the zwitterionic Cy3NOS interacts with the nucleotides more than the anionic Cy3. Comparing spectra of equimolar solutions of probe 56NOS when single-stranded and double-stranded (Fig. 7C), one notes that the shoulder at 310 nm decreases upon addition of DNA target. This is the behavior that one would expect since the formation of the double helix should disrupt the dye–nucleotide interactions. In addition, the double-stranded absorbance spectrum of 56NOS (Fig. 7C) begins to look very similar to the composite spectrum of probe 56NOS when no dye–nucleotide or dye–dye interactions are present (Fig. 7B), indicating that duplex formation disrupts dye–dye, as well as dye–nucleotide, associations.

Therefore, it appears that both dye–dye and dye–nucleotide interactions are present. If the dye–nucleotide and dye–dye interactions are strong enough, then the duplex should be destabilized by those interactions, which seems to be the case. The relative

contributions of the dye–dye and dye–nucleotide interactions to the destabilization of the hybridized probes will be probe-dependent. Dye–dye interactions will be favored at higher labeling densities and when longer linkers are used. Though dye dimers are known to quench fluorescence (33), it is possible that dye–nucleotide interactions may enhance it. It is known that increasing the planarity of cyanine dyes leads to an increase in the Φ_f (32). Therefore, if dye–nucleotide interactions stabilize a planar dye conformation, they may also enhance fluorescence. If this is true, then the balance between fluorescence quenching effects from dye–dye interactions and fluorescence enhancement effects from dye–nucleotide interactions may account for the complicated behavior seen in Figure 5.

CONCLUSION

In this study, we synthesized a series of multiply-labeled fluorescent oligonucleotides. We investigated the effect of labeling density, fluorophore charge and linker length upon fluorescence intensity, the change in fluorescence upon duplex formation, the quantum yield of fluorescence, probe–target stability and specificity to determine *in vitro* the best probe. Our work indicates that (i) the optimum *in vitro* probe is obtained when labeling with a hydrophilic dye such as Cy3 every 6th base using a long linker; (ii) the probe–target duplex formed is less stable for multiply-labeled fluorescent DNA probes due to dye–dye and dye–nucleotide interactions which appear to stabilize a single-stranded conformation of the probe; (iii) the target specificity is just as high as compared to the unmodified control probe.

In designing multiply-labeled fluorescent DNA probes, our work suggests that the primary concern should be to optimize the brightness of the probe while maintaining its ability to form a stable duplex. In optimizing probe brightness, one should begin with the design of the fluorophore itself since the optimum labeling density depends upon the fluorophore used. Future fluorophore development should focus on reducing the tendency of dyes to form these aggregates since it is dye–dye and dye–nucleotide aggregation which lowers the stability of the probes as well as their fluorescence brightness. If this can be achieved while maintaining high extinction coefficients and quantum yields, then the sensitivity of the resulting probes would be greatly enhanced.

Aggregation can be inhibited by increasing the hydrophilicity of the fluorophore or modifying it with bulky groups that sterically interfere with dimerization. For indocarbocyanines, sulfonation of the indolenine rings has been shown to be a very effective approach since the sulfonate groups are very bulky while adding hydrophilicity to the dye. This has led to the exceptional qualities of Cy3 for which the Φ_F doubles upon conjugation to an oligonucleotide; for comparison, the Φ_F of a fluorescein-conjugated oligonucleotide decreases by 85% (35). This makes the Cy3-labeled DNA probe approximately twice as bright as a fluorescein-labeled conjugate, with brightness defined as $\varepsilon \cdot \Phi_F$. Other approaches, such as encapsulation in cyclodextrins, are currently under investigation.

ACKNOWLEDGEMENTS

We are indebted to Dr James Franzen of the University of Pittsburgh and Dr Klaus Hahn of the Scripps Research Institute for their generous help and insightful discussions. This work was supported by NSF grant MCB-8920118.

REFERENCES

1 Birchall,P.S., Fishpool,R.M. and Albertson,D.G. (1995) *Nature Genet.* **11**, 314–320.
2 Senatorov,V.V., Trudeau,V.L. and Hu,B. (1995) *Brain Res. Mol. Brain Res.* **30**, 87–96.
3 Yu,H., Ernst,L., Wagner,M. and Waggoner,A. (1992) *Nucleic Acid Res.*, **20**, 83–88.
4 Pennline,K.J., Pellerito-Bessette,F., Umland,S.P., Siegel,M.I. and Smith,S.R. (1992) *Lymphokine Cytokine Res.* **11**, 65–71.
5 Dao,D.D., Sawyer,J.R., Epstein,J., Hoover,R.G. and Barlogie,B. (1994) *Tricot. G. Leukemia* **8**, 1280–1284.
6 Martinez-Climent,J.A., Thirman,M.J., Espinosa,R.,III, Le Beau,M.M. and Rowley,J.D. (1995) *Leukemia* **9**, 1299–1304.
7 Veronese,M.L., Ohta,M., Finan,J., Nowell,P.C. and Croce,C.M. (1995) *Blood*, **85**, 2132–2138.
8 Kraker,W.J., Borell,T.J., Schad,C.R., Pennington,M.J., Karnes,P.S., Dewald,G.W. and Jenkins,R.B. (1992) *Mayo Clin. Proc.* **67**, 658–662.
9 Fujii,M., Ogata,T., Takahashi,E., Yamada,K., Nakabayashi,K., Oishi,M. and Ayusawa,D. (1995) *FEBS Lett.* **375**, 263–267.
10 Lawrence,J.B., Villnace,C.A. and Singer,R.H. (1988) *Cell*, **52**, 51–61.
11 Pinkel,D., Straume,T. and Gray,J.W. (1986) *Proc. Natl. Acad. Sci. USA* **83**, 2934–2938.
12 Smith,L.M., Sanders,J.Z., Kaiser,R.J., Hughes,P., Dodd,C., Connell,C.R., Heiner,C., Kent,S.B. and Hood,L.E. (1986) *Nature* **321**, 674–679.
13 Prober,J.M., Trainor,G.L., Dam,R.J., Hobbs,F.W., Robertson,C.W., Zagursky,R.J., Cocuzza,A.J., Jensen,M.A. and Baumeister,K. (1987) *Science* **238**, 336–341.
14 Connolly,B.A. (1987) *Nucleic Acids Res.* **15**, 3131–3139.
15 Yu,H., Chao,J., Patek,D., Mujumdar,R., Mujumdar,S. and Waggoner,A.S. (1994) *Nucleic Acids Res.* **22**, 3226–3232.
16 Folsom,V., Hunkeler,M.J., Haces,A. and Harding,J.D. (1989) *Anal. Biochem.* **182**, 309–314.
17 Haralambidis,J., Chai,M. and Tregear,G.W. (1987) *Nucleic Acids Res.* **15**, 4857–4876.
18 Brumbaugh,J.A., Middendorf,L.R., Grone,D.L. and Ruth,J.L. (1988) *Proc. Natl. Acad. Sci. USA* **85**, 5610–5614.
19 Singh,D., Vijayanti,K. and Ganesh,K.N. (1990) *Nucleic Acids Res.* **18**, 3339–3345.
20 Wallner,G., Amann,R. and Beisker,W. (1993) *Cytometry* **14**, 136–143.
21 West,W., Pearce,S. and Grum,F. (1967) *J. Phys. Chem.* **71**, 1316–1326.
22 Levinson,G.S., Simpson,W.T. and Curtis,W. (1957) *J. Am. Chem. Soc.* **79**, 4314–4320.
23 Mineno,J., Ishino,Y., Ohminami,T. and Kato,I. (1993) *J. DNA Seq.* **4**, 135–141.
24 Aurup,H., Tuschl,T., Benseler,F., Ludwig,J. and Eckstein,F. (1994) *Nucleic Acids Res.* **22**, 20–24.
25 Ozaki,H. and McLaughlin,L.W. (1992) *Nucleic Acids Res.* **20**, 5205–5214.
26 Wang,S., Friedman,A.E. and Kool,E.T. (1995) *Biochemistry* **34**, 9774–9784.
27 Mujumdar,R.B., Ernst,L.A., Mujumdar,S.R., Lewis,C.J. and Waggoner,A.S. (1993) *Bioconjugate Chem.* **4**, 105–111.
28 Maniatis,T., Fritsch,E.F. and Sambrook,J. (1989) *Molecular Cloning: A Laboratory Manual.* Cold Spring Harbor Laboratory Press, Cold Spring Harbor, NY.
29 Cantor,C.R. and Tinoco,I. (1965) *J. Mol. Biol.* **13**, 65–77.
30 Fasman,G.D. (ed.) (1975) *Handbook of Biochemistry and Molecular Biology.* 3rd Ed. Vol. 1. CRC Press, Inc., Cleveland, OH.
31 Franzen,J.S., Zhang,M., Chay,T.R. and Peebles,C.L. (1994) *Biochemistry,* **33**, 11315–11326.
32 O'Brien,D.F., Kelly,T.M. and Costa,L.F. (1976) *Photogr. Sci. Engng.* **18**, 76–84.
33 Herz,A.H. (1974) *Photogr. Sci. Engng.* **18**, 323–335.
34 Vàmosi,G., Gohlke,C. and Clegg,R.M. (1996) *Biophys. J.* **71**, 972–994.
35 Telser,J., Cruickshank,K.A., Morrison,L.E. and Netzel,T.L. (1989) *J. Am. Chem. Soc.* **111**, 6966–6976.